論文内容の要旨

論文題目: Observational study on the self-similarity of earthquake rupture growth in Parkfield area

(パークフィールド地域における震源破壊成長の自己相似性について)

氏名　内出 崇彦

Introduction

The similarity and dissimilarity between the rupture growths of large and small earthquakes is quite interesting and essential issue in not only earthquake seismology but also disaster prevention by earthquake early warning. To address this issue, there have been so many scaling studies of rupture processes of earthquakes. However most of them were on the source parameters in the eventual state of earthquakes, such as fault dimensions, average fault slip, average stress drop, source duration, and so on.

Now we focus on the scaling of earthquake rupture growth (temporal development of earthquake rupture), which has been rarely done. In this thesis, we analyze six earthquakes in a wide magnitude range, M_W 1.7 – 6.0, by slip inversion analyses. And, based on the comparison of their rupture process in terms of their moment rate and cumulative moment functions, we discuss on earthquake rupture growth.

Multiscale slip inversion

Slip inversion analysis is very useful to reveal an earthquake rupture growth process. However ordinary slip inversion analyses cannot resolve the very beginning of rupture process. Therefore, we developed a multiscale slip inversion algorithm [*Uchide and Ide*, 2007] employing a multiscale source model which is constructed by renormalizing source models with different node intervals and fault dimensions. Our multiscale approach enables to investigate the early stage and the whole processes of an earthquake in detail simultaneously.

Multiscale slip inversion of the 2004 Parkfield earthquake

Focusing on the early stage of a large earthquake, we investigate the 2004 Parkfield earthquake (M_W 6.0) by the multiscale slip inversion analysis, reviewed in the previous section. The data of GEOS and CGS strong-motion network are in use. The employed multiscale source model is composed of three models at different scales. For the smaller two scales, we construct empirical Green's functions from observed waveforms of three earthquakes each. For the largest scale, we calculate Green's functions by assuming a layered crust structure.

Our multiscale approach successfully reveals a detailed image in the early stage of the large earthquake together with the entire rupture process (Figure 2). From its very onset, the rupture is complex with a high slip rate and high rupture propagation speed. Rupture begins bilaterally, and the rupture velocity is about 3.0 km/s and slip-rate is as high as 3 m/s even at 0.2 s, though our resolution within the first 0.1 s is limited. The high-speed initial rupture inferred from our model is consistent with that of the 2004 mid-Niigata Prefecture, Japan, earthquake (M_W 6.6) [*Uchide and Ide*, 2007], which implies that such characteristics may be quite general.

At the 0.2 s from the onset, the cumulative seismic moment is equivalent to M_W 3.9, and only 0.1 % of the eventual seismic moment. Is this high-speed rupture process in the early stage identical to medium earthquakes, such as M_W 4 – 5? This problem will be approached in the next section by comparing earthquake growth process of earthquakes with different final sizes.

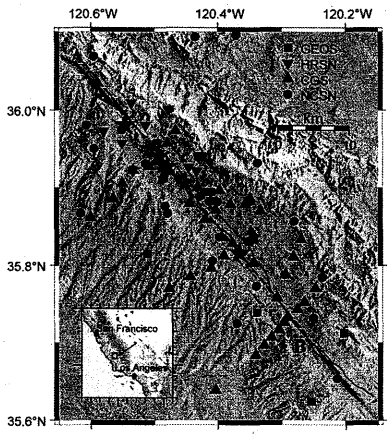

Figure 1
Map of Parkfield area. Squares, inverted triangles, normal triangles indicate the station location. Stars indicate the epicenter of earthquakes we investigate.

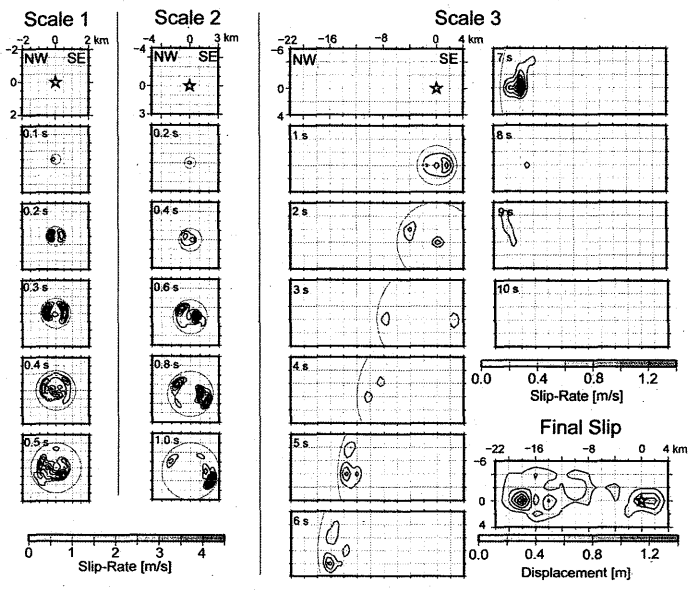

Figure 2
Slip-rate distribution history and final slip distribution of our preferred multiscale fault model. The gray circles indicate the hypothetical rupture front, within which slip is allowed, propagating at 3.0 km/s from the hypocenter.

Scaling of earthquake rupture growth

Next we investigate the rupture process of five earthquakes (M_W 1.7 – 4.6) by standard (not multiscale) slip inversion analyses employing data of GEOS and HRSN and empirical Green's functions, for the comparison with the M_W 6.0 event studied in the previous section.

Figure 3 shows scaled moment rate functions of the six earthquakes studied, where time and moment rate is scaled by a reference source duration, $T_o = 2.7\times10^{-6} M_o^{1/3}$ (M_o is the final magnitude), and average moment rate, M_o/T_o, respectively. The moment rate functions of all earthquakes except M_W 6.0 event are similar to each other and approximately symmetric bell-shaped. We term the process before the peak (or earlier half of rupture process) "growth stage," and that after the peak (or latter half) "decline stage." On the other hand, the scaled moment rate function of M_W 6.0 event is quite different from others, and almost constant at a much lower level than the peaks of other events.

The representative figure of this thesis is Figure 4, which shows the cumulative moment functions of six earthquakes we investigated in a log-log graph. For all events in their growth stages, the cumulative moment functions increase along a common growth line, $M_o(t) = 2\times10^{17} t^3$, independent of its eventual magnitude. The proportionality of the cumulative moment to the cube of the time from the onset implies the self-similarity of earthquake rupture growth. According to the self-similar model, the proportionality coefficient is proportional to the stress drop and the cube of the rupture propagation speed.

The cumulative moment function of the M_W 6.0 earthquake shows the break of t^3-proportionality at 1 s, after which the cumulative moment function is roughly proportional to the time. That is likely because the rupture was suppressed by the finite thickness of a seismogenic layer by following reasons. Figure 5 shows the final slip distribution of the M_W 6.0 event and the seismicity on the San Andreas Fault. According to the seismicity, the thickness of the seismogenic layer around the hypocenter of the M_W 6.0 event is limited within 5 – 10 km in depth. The slip of the M_W 6.0 is confined within the estimated seismogenic layer, though the assumed source models included the shallower part of the San Andreas Fault. The time of the break of t^3-proportionality, 1 s, is comparable to the time when the rupture front reached at the top and bottom of the seismogenic layer around the hypocenter. The effect of the finite thickness of the seismogenic layer produces the difference between the scaled moment rate functions of M_W 6.0 and other smaller earthquakes.

The rupture process of the M_W 6.0 earthquake before 1 s and the entire rupture processes of other smaller earthquakes appear not to be affected by the limitation of the seismogenic zone. Besides the rupture process in the growth stage seems not to be dependent on its own final size. These implications are probably because small rupture involves only a surrounding small zone. The magnitude of earthquakes is not determined before the deceleration, but by chance. Therefore the switch to the decline stage is probably important for determining the eventual magnitude of an

earthquake. For the estimation of the eventual magnitude on the purpose of earthquake early warning, we should wait for, at least, the transition from the growth stage to the decline stage.

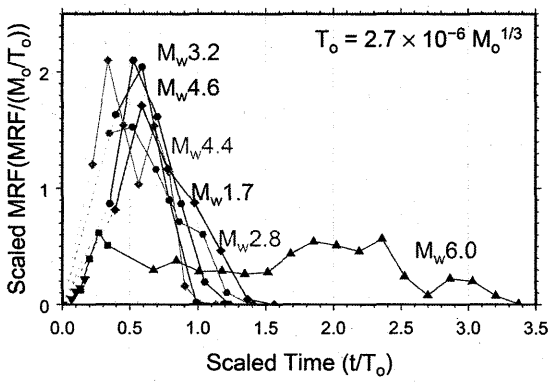

Figure 3
Scaled moment functions of the six target events (M_W 1.7 – 6.0). Time and moment rate are normalized by T_o and M_o/T_o, respectively, where $T_o = 2.7 \times 10^{-6} M_o^{1/3}$ and M_o is the final seismic moment of each event.

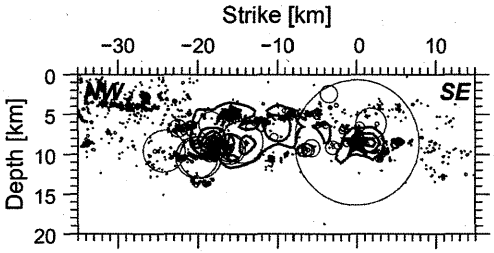

Figure 5
Slip distribution of the M_W 6.0 event (red contours; contour interval is 0.2 m) and hypocenters (grey circles; January 1, 1984 – June 30, 2005; relocated by *Thurber et al.* [2006]) on the cross section at San Andreas Fault.

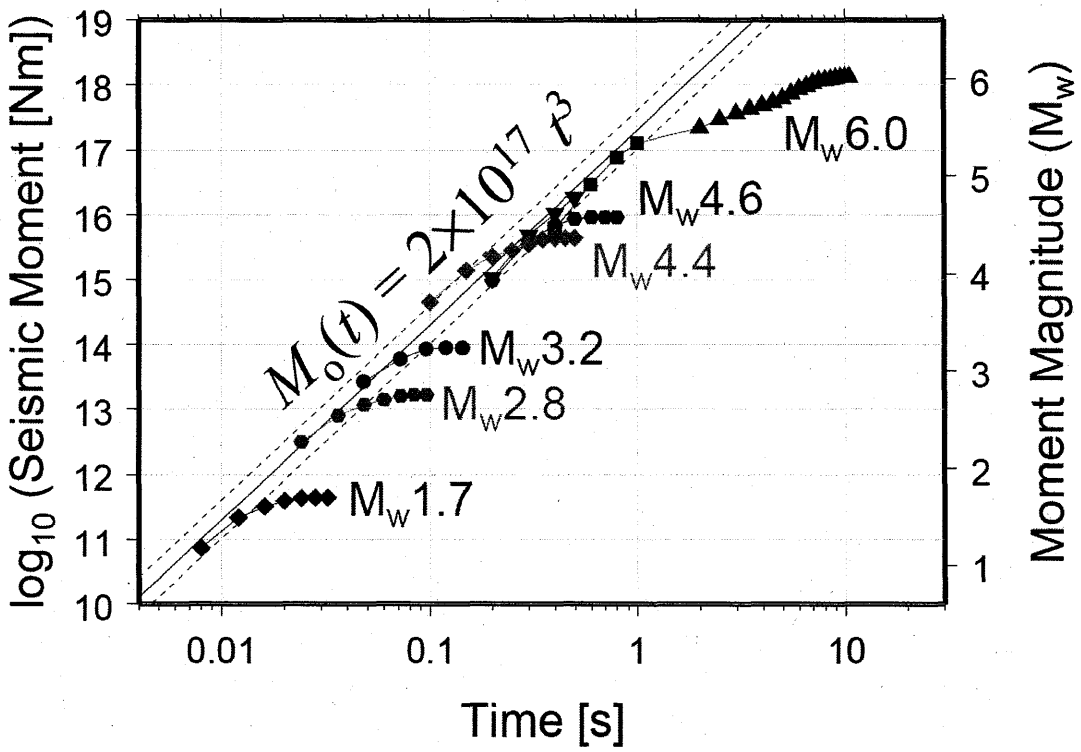

Figure 4
Cumulative moment functions of six target events (M_W 1.7 – 6.0) in the log-log graph. Intervals of points are same as the node intervals of the source models.